Mathematical Modelling and Numerical Simulation with Applications, 2024, 4(3), 370–394

https://dergipark.org.tr/en/pub/mmnsa
ISSN Online: 2791-8564 / Open Access
https://doi.org/10.53391/mmnsa.1517843

RESEARCH PAPER

A seismic-risk-based bi-objective stochastic optimization framework for the pre-disaster allocation of earthquake search and rescue units

Nadi Serhan Aydın [1,*,‡]

[1]Department of Industrial Engineering, Faculty of Engineering and Natural Sciences, Istinye University, Sarıyer 34396, Istanbul, Türkiye

* Corresponding Author
‡ serhan.aydin@istinye.edu.tr (Nadi Serhan Aydın)

Abstract

Accurately predicting earthquakes' time, location and size is nearly impossible with today's technology. Severe earthquakes require prompt and effective mobilization of available resources, as the speed of intervention has a direct impact on the number of people rescued alive. This, in turn, calls for a strategic pre-disaster allocation of search and rescue (SAR) units, both teams and equipment, to make the deployment of resources as quick and equitable as possible. In this paper, a seismic risk-based framework is introduced that takes into account distance-based contingencies between cities. This framework is then integrated into a mixed-integer non-linear programming (MINLP) problem for the allocation of SAR units under uncertainty. The two minimization objectives considered are the expected maximum deployment time of different SAR units and the expected mean absolute deviation of the fulfillment rates. We recover the best vulnerability-adjusted routes for each size-location scenario as input to the optimization model using the dynamic programming (DP) approach as part of the broader area of reinforcement learning (RL). The results of the hypothetical example indicate that the comprehensive model is feasible in various risk scenarios and can be used to make allocation-deployment decisions under uncertainty. The results of the sensitivity analysis verify that the model behaves reasonably against changes in selected parameters, namely the number of allowed facilities and weights of individual objectives. Under the assumption that the two objectives are equally important, the model achieves a total deviation of 3.5% from the objectives with an expected maximum dispatch time of 1.1327 hours and an expected mean absolute deviation of 0.01%.

Keywords: Earthquake response; SAR units allocation; mixed-integer nonlinear programming (MINLP); stochastic optimization; dynamic programming

AMS 2020 Classification: 90B06; 90C11; 90C15; 90C39

➤ **Received:** 17.07.2024 ➤ **Revised:** 26.09.2024 ➤ **Accepted:** 29.09.2024 ➤ **Published:** 30.09.2024

1 Background

Disasters due to natural hazards rarely occur, but once they occur, they can cause extreme fatalities and physical damages. World Health Organization (WHO) estimates that, between 1998-2017, earthquakes claimed nearly 750,000 lives worldwide, which is more than 50% of all deaths related to natural disasters [1]. Disaster risk from earthquakes can be mitigated by decreasing both the exposure of the property to active fault zones and its fragility. On the other hand, the effects of SAR on disaster fatality have long been recognised and explored (see, e.g., [2, 3]). That being said, there is also a need for effective pre-disaster allocation of search-and-rescue (SAR) units for the response to the earthquake to be timely and life-saving. It is a well-known fact that the likelihood of finding survivors in any location is inversely related to time [4]. Research has shown that many more victims could survive if medical care in SAR was provided quickly and effectively [5]. With data collected from the China Earthquake Database for 51 earthquakes globally, Figure 1 aims to highlight the difference in SAR efficiency for earthquakes with different scales, where the completion ratio denotes the ratio of cumulative death toll up to the current time to the final death toll. It is clear that larger-scale earthquakes are associated with slower growth in the percentage of victims reached, thus lower SAR efficiency, especially during the *golden 72 hours* into the earthquake's occurrence. This implies that there is an ample room for improving SAR efficiency by making a better use of the available resources. The efficient planning of SAR operations has a significant role in saving lives in the response phase to disasters [6]. To guarantee an adequate and timely response, effective prepositioning of different SAR units to certain locations and in certain quantities is crucial [7].

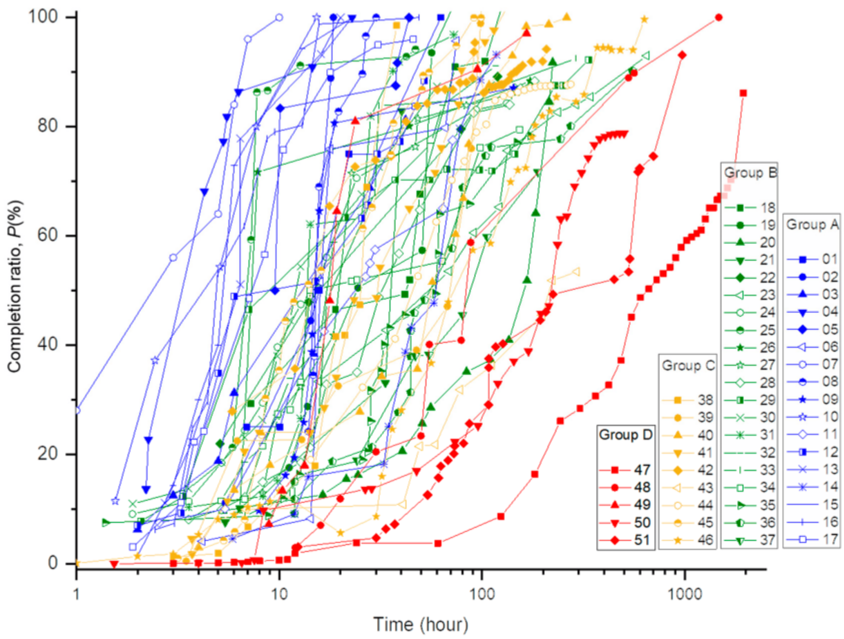

Figure 1. SAR completion ratio curves for the reported death tolls in earthquakes globally [8] (Groups A-D represent earthquakes with death tools < 100, $100 - 1,000$, $1,000 - 10,000$ and $> 10,000$, respectively)

All in all, disaster risk management problems are strongly characterized by random outcomes, which indicates the importance of using mathematical tools that can thoroughly take into account the stochastic nature of these problems [9]. In this study, our primary focus is on the humanitarian losses due to devastating earthquakes, and we classify the latter mainly into the following groups:

- Those captured under and lost lives immediately after the earthquake happens due to collapse

of buildings,
- Those captured under and lost lives after a period since they could not be rescued on time,
- Those rescued from wreckage but could not been hospitalized timely.

As only the losses belonging to the second and third group are preventable with the collective availability of rescue entities (i.e., rescue teams, ambulances, and heavy equipment), the present study seeks to optimize the pre-disaster allocation of SAR units through minimizing two objectives, namely, the expected maximum time it takes to dispatch all needed SAR units and the expected mean percentage deviation of fulfillment rates across all cities.

In this regard, starting from a fault map, the present study focuses on designing a pre-disaster framework for allocating disaster rescue teams and equipment with a view to minimizing both the maximum of the average delivery times associated with each SAR unit type to entire earthquake region and absolute deviation of fulfillment rates across cities. The first objective can be justified by the reasonable assumption that entities will largely be dysfunctional without one another. To give an example, rescue teams without excavators, ambulances without rescue teams, or excavators without ambulances will not be able to perform their functions. Therefore, one entity can start performing its rescue action only after other entity types arrive. This, in turn, calls for the minimization of the longest time period it takes for a specific entity to arrive at the disaster site. The second objective, on the other hand, will ensure that SAR units will not be clustered in one location to prioritize only the city with highest conditional disaster risk.

The study aims to develop an integrated and flexible framework for SAR unit allocation and deployment, combining a seismic risk framework similar to that in [10] with a MINLP model to achieve the joint objective of minimizing the dispatch time of SAR units and variation between response rates. Particularly, the incorporation of seismic risk components and consideration of conditional damage on infrastructure to calculate shortest routes constitute significant research gaps that the present study seeks to address. The rest of the study is organized as follows: Section 2 offers a summary of the related literature. Section 3 provides the details of the risk-based model, including the seismic hazard framework as well as the DP model for recovering vulnerability-adjusted shortest routes and the main MINLP model. Section 4 presents a numerical example on the comprehensive model introduced in Section 3. In Section 5, we give results and the related discussion. Section 6 then concludes.

2 Related literature

The literature on planning the allocation and displacement of earthquake SAR units is broad and focuses on a variety of methods ranging from mixed integer programming (MIP) to stochastic programming and meta-heuristics. Fairly comprehensive reviews of the literature on the use of optimization methods in disaster response are presented, e.g., in [11–13]. We refer the interested reader to these studies.

Stochastic programming

Authors such as, but not limited to, [14–18] presented stochastic programming (SP) models, some of which are multi-stage. For example, [14] applied multi-stage SP for deploying urban search and rescue teams with a view to maximizing the total expected number of people rescued. To make the model more realistic, the likelihood of survival is assumed to diminish over time. Using a two-stage model, [15] sought to minimize the total cost of facility location, inventory holding, transportation and shortage in the context of a humanitarian relief problem. [18] proposed a tri-objective model for pre-and post-earthquake decisions, whereas a novel multi-objective particle swarm optimization (PSO) algorithm was used for solving the model. [17] introduced a stochastic multi-objective mixed-integer mathematical programming logistic distribution and evacuation planning during earthquake. [19] used a stochastic modeling framework to incorporate various uncertainties such as facility damage and casualty losses as a function of the magnitude of the earthquake, and developed an evolutionary optimization *heuristic* aided by an innovative mixed integer programming (MIP) model that was used to initialize the algorithm. The model was showcased with an application to a region that is prone to earthquakes.

Integer programming

Some other authors like [20–22] opted for pure integer programming (IP) models −linear or non-linear− to tackle the allocation problem. [21] proposed an integer nonlinear multi-objective, multi-period, multi-commodity model to minimize the travel time and total cost and increases reliability of the routes from distribution centers. [20] employed a multi-objective integer nonlinear programming model for assigning rescue teams to disaster sites. The model aimed to minimize the maximum arrival time of all rescue teams to the affected areas and, at the same time, maximize the satisfaction of rescue teams for their assignments. Methods such as NSGA-II, C-METRIC and fuzzy logic were then used to solve the model. The model was then applied to a real earthquake event. [23] combined simulation with a two-phase IP model whereby the first phase aimed to minimize the total distance to be covered for distributing relief supplies by determining the optimal amount of these supplies each neighborhood sent and/or received and, the second phase, to minimize the total number of facilities. [24] proposed a two-stage robust scenario-based optimization problem to facilitate decisions regarding, inter alia, suitable locations for shelters, the optimal route for evacuating people, total rescue time, required budget. NSGA-II was proposed as the solution method. [25] designed a bi-objective robust mixed-integer linear programming (MILP) model for rescue units' allocation and scheduling also by considering the learning feature of rescue units. [6] offered a robust decision support framework for post-earthquake planning SAR resource deployment. In this regard, a two-stage MIP-based decomposition approach was proposed where the first phase performs the allocation of SAR units for maximizing fair and effective demand coverage and the second phase deals with the routing of resources with the aim of minimizing the weighted sum of fulfillment times. [26] developed a decision support model, namely, a MINLP, that minimizes the sum of completion times of incidents weighted by their severity and compared several *heuristics* and *meta-heuristics*.

Other modelling approaches

In [27], a dynamic combinatorial optimization model was introduced to find the best assignment of available resources to operational areas, thereby minimizing the total number of fatalities. First three days after an earthquake takes place were considered to be essential to the success of relief efforts. *Heuristics*, namely, Simulated Annealing (SA) and Tabu Search (TS), were used to solve the model. [28] presented a simulation-based approach for probabilistic modelling to improve post-disaster relief and recovery operations.

Incorporating a seismic-risk model

[10] presented a risk-based approach that incorporates hazard, exposure and vulnerability data, for the pre-positioning of relief resources in appropriate locations. Again, a MILP model used in the study aimed to allocate assets to the locations with the highest levels of risk and then minimize the residual risk. Applying the model on 87 counties Wyoming and Colorado, US, authors reported an at least 33% improvement in residual risk when compared to historical allocations. [7] proposed a two-phase framework based on a compound stochastic process that models' disaster attributes

such as occurrence time, intensity and severity. [29] developed a machine learning framework to predict the casualty rate and direct economic loss induced by earthquakes. They found earthquake magnitude, position, and population density to be the leading indicators for loss prediction.
Table 1-Table 2 summarize the relevant literature in a tabular format and in comparison with the present work. Against this background, methodological as well as managerial contributions of the current study can be outlined as follows. Unlike the majority of the previous studies, this paper:

- Presents an integrated and flexible approach that can be adapted to various hazard / fragility / exposure scenarios. Yet, the model's ability to adapt is partly undermined by
- Links the resource allocation and dispatching problem to a seismic risk modelling framework. This aspect is missing from a vast majority of the studies reviewed.
- Incorporates vulnerability-adjusted shortest routes into the problem for more realistic resource allocation. This is achieved through identifying post-disaster optimal routes for each possible scenario through dynamic programming.
- Helps policymakers make more equitable earthquake dispatchment decisions by understanding its marginal impact on the speed of dispatchment. This aspect is also usually omitted in the existing literature.

3 Model description

In this paper, we apply a seismic-risk-based stochastic bi-objective pre-disaster resource allocation framework modelled as a mixed-integer non-linear programming (MINLP) model, starting from the formulation of a seismic hazard framework and incorporating the vulnerability of cities through fragility curves. The framework deals with the question of how the available SAR resources should be located throughout an earthquake zone, with a view to minimizing not only the expected maximum time it takes for each SAR unit type to be dispatched to the cities affected but also the expected mean absolute deviation of fulfillment rates across cities.
More specifically, we present a stochastic resource allocation model that takes the map of existing fault lines on an IxJ grid, with their hazard (i.e., probability) of producing an earthquake with a certain demand parameter g in the planning period (e.g., 10 years) as input and decides on the optimal allocation of SAR units to facilities and dispatch of these units to earthquake zones based on the realized scenarios, and taking into account their post-earthquake accessibilities which will be affected by potential damages in the transportation infrastructure.
SAR units considered in this study consist of 4 types: rescue teams, excavators or bulldozers, trucks, and ambulances. These units are needed to make the first intervention in any earthquake rescue operation. As explained later, the number of available units from each type k will be set to the conditionally expected number of collapsed buildings (i.e., conditional risk of disaster) provided that an earthquake occurs, multiplied by a factor α_k that determines the quantity of equipment needed per collapsed building.
We start by introducing fault zones $z \in \mathcal{Z}$ where fault zone z has n_z fault segments, each with a city on it. A fault segment will be activated during a seismic event and cause an earthquake with a peak ground acceleration (PGA) value $g \in \mathcal{G}$.[1] Each segment on a fault zone is assumed to have even probability of being epicenter to an earthquake. When an earthquake occurs, it is known that the *hazard* of natural disaster is transformed into the *risk* of environmental / economic / social disaster through vulnerability (or fragility) of cities and property stock's level of exposure. Fragility curves, in this regard, are widely used to associate the demand parameter of the earthquake with the

1 ground motion, of which PGA is a measure, is argued to be related more closely to the level of damage to buildings and infrastructure in an earthquake, rather than the magnitude of the earthquake itself.

Table 1. Tabular literature and present study

Citation	Disaster phase	Optimization model	Uncertainty handling	Seismic model	Decision	Objective	Solution method/tool	Case study / example
This study	Pre/post	Stochastic programming model (nonlinear)	Stochastic	Yes	Locate SAR facilities and dispatch SAR units	Minimize maximum dispatch time; minimize mean absolute deviation between fulfillment rates	Sample Average Approximation	Numerical
[24]	Post	Two-stage multi-objective multi-period robust scenario-based optimization model	Robust opt.	None	Locate temporary shelters and assign injured people to the shelters	Minimize time and the cost of the relief operation in various scenarios	NSGA-II	Real (Tehran, Iran)
[6]	Post	Two-stage MILP model	Robust opt.	None	Robust allocation and routing of search and rescue resources	Maximize the demand coverage for the district with the lowest coverage score (minimize the gap between coverage scores)	Direct	Scenario (Tehran, Iran)
[30]	Pre	Scenario-based stochastic program (non-linear)	Stochastic	None	Storage facility location and material prepositioning decisions (pre-disaster) and service allocation (post-disaster)	Minimize total system costs across all scenarios (facility set-up cost, material prepositioning cost, transportation cost, and victims' deprivation cost)	Direct	Numerical (US)
[17]	Pre/post	Stochastic multi-objective mixed-integer mathematical programming	Stochastic	None	Location of distribution and care centers, amount and distribution of commodities	Minimize expected value of maximum weighted percentage of untreated injured people	Chance constraint; epsilon-constraint, NSGA-II	Real (Tahran, Iran)
[25]	Post	Bi-objective mixed-integer linear programming (MILP) model	Robust opt.	None	Allocating and scheduling disaster rescue units	Minimize total weighted time to complete all the rescue operations; minimize the total weighted delay in all the rescue operations	Multi-choice goal programming	Mazandaran, Iran
[10]	Pre	Mixed-integer programming model (linear)	Probabilistic	Yes	Pre-positioning of relief resources in appropriate locations	Minimize the sum of the residual risk values across the entire overall region	Direct	Colorado /Wyoming

Table 2. Tabular literature and present study (cont'd)

[31]	Pre, post	Bi-level stochastic optimization model	Stochastic	None	budget allocation for improving the efficiency of the transportation network in pre- and post-disaster	Minimize the overall network travel time; minimize the expected number of casualties	Particle Swarm Optimization (PSO)	Numerical
[7]	Pre	Two-stage stochastic programming model	Stochastic	Yes	Location, number and capacity of distribution centres, and quantity of emergency items to keep	Minimize total transportation and procurement costs; minimize total penalty associated with satisfying demands	Monte Carlo, Sample Average Approximation	North Carolina, US
[21]	Post	Integer nonlinear multi-objective, multi-period, multi-commodity model	None	None	Locate distribution centers for timely distribution of relief, vehicles routing and emergency roadway repair operations	Minimize maximum vehicle route traveling time; minimize total cost; maximize minimum reliability of route	NSGA-II, MOPSO	Test problems
[20]	Post	Multi-objective multistage integer nonlinear programming model	None	None	Emergency rescue team assignment in the disaster chain	Minimize maximum arrival time of all rescue teams to affected areas; maximize satisfaction of rescue teams assignment	NSGA-II, C-METRIC and fuzzy logic	Wenchuan, China
[18]	Pre, post	Three-objective stochastic programming model	Stochastic	None	Numbers and locations of distribution centres, stocking levels of relief items, commodity flow amounts	Maximize total expected demand coverage; minimize total expected cost; minimize difference in satisfaction rates	MOPSO, NSGA-II	Tehran, Iran
[19]	Pre	Stochastic optimization model	Stochastic	No	Location and capacity of distribution centers	Minimize total expected costs (facilities, supplies and fatalities) by determining the capacity and location of DCs	MIP (initial solution) and evolutionary heuristics	Los Angeles, California, US
[22]	Pre	Mixed-integer programming (MIP) model / network flow model	None	None	Locate and allocate temporary distribution centers in different time periods	Minimize logistics and penalty costs	Direct	South Carolina, US

conditional probability of a certain damage state (e.g., total damage or collapse) occurring.
As stated earlier, the objective of our model is to minimize the preventable humanitarian losses through the optimal allocation of SAR units to have them timely and equitably dispatched to disaster sites. As the preventable losses increases with time due to lack of SAR units and as different types of units have to work together (*inter-dependence*), our objective of *timeliness* will be based on shortening the arrival time of the latest-arriving SAR unit type.
Severe earthquakes are extremely rare events yet with huge conditional impact. One challenge for policymakers is therefore to decide on the quantity of SAR units to be kept available at SAR facilities. A conservative but unrealistic strategy is to make available the amount of equipment that is adequate for the worst-case size-location scenario assuming that it will materialize. An alternative yet opposite approach would be based on the unconditional risk of disaster. A flowchart of the modelling methodology followed in this paper in presented in Figure 2. We first introduce a seismic risk methodology based on hazard, vulnerability and exposure maps. This framework provides conditional risk values (expected demand for SAR units) as an input to the bi-objective optimization model, whereas the conditional shortest routes are served by the DP model for each earthquake scenario and city pair. The optimization model is then solved using the weighted sum approach and for different values of the selected parameters.

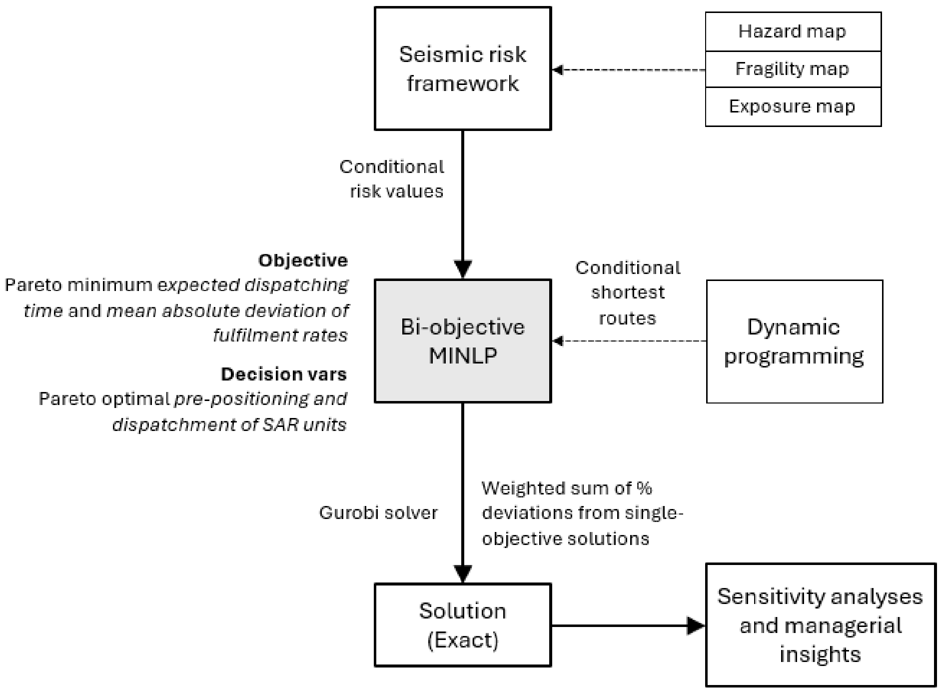

Figure 2. Methodology flowchart

Mathematical model

Model assumptions, sets and indices

Model assumptions that are made to avoid some undesired complexities can be stated as follows:

i. Each city will have at most one earthquake over the planning period,
ii. Earthquakes are independent among fault zones, i.e., they will not happen around the same time,
iii. A break can occur at any segment of a fault zone with even probability,
iv. Each city can only be in a single fault zone,

v. The Impact of an earthquake on a city is homogeneous,
vi. Distribution of the residential property stock in a city is homogeneous,
vii. Residential properties have an equal number of independent units each with an equal number of residents,
viii. SAR facilities and units are not affected by the earthquake,
ix. There is no setup time or minimum batch size for SAR units to mobilize.

The sets, indices and parameters related to the model are given in Table 3 and Table 4.

Table 3. Sets and indices

i :	Index of vertical coordinate ($i \in \mathcal{I}$ where $\mathcal{I} = \{1, 2, \ldots, I\}$)
j :	Index of horizontal coordinate ($j \in \mathcal{J}$ where $\mathcal{J} = \{1, 2, \ldots, J\}$)
f :	Index of facilities ($f \in \mathcal{F}$ where $\mathcal{F} = \{f_1, f_2, \ldots\}$)
c :	Index of cities ($c \in \mathcal{C}$ where $\mathcal{C} = \{c_1, c_2, \ldots\}$)
k :	Index of equipment types ($k \in \mathcal{K}$ where $\mathcal{K} = \{k_1, k_2, \ldots\}$)
s :	Index of spatial states of earthquake ($s \in \mathcal{S}$ where $\mathcal{S} = \{s_1, s_2, \ldots\}$)
g :	Index of PGA states of an earthquake ($g \in \mathcal{G}$ where $\mathcal{G} = \{g_1, g_2, \ldots\}$)
ξ_z :	Sets of fault zones ($z \in \mathcal{Z}$ where $\mathcal{Z} = \{1, 2, \ldots, Z\}$) indicating cities in the fault zone

Table 4. Parameters

n_z	Number of cities located on fault zone ξ_z
n_F^k	Number of facilities allowed for SAR unit type k
Av_k	Number of available SAR units of type k
β_c	Current building stock in city c
α_k	The number of SAR unit type k needed for each collapsed building
v_k	Average velocity (in 100 mph) of SAR unit type k under normal conditions

Seismic risk framework

Let n_z be the number of cities on the fault zone z. Assuming that the fault zone can fail in any part of it with even probability, the hazard of city c on fault zone z for being the epicenter to a devastating earthquake with a demand parameter g can be defined as

$$EP_{cg} = I_{\{c \in \xi_z\}} \frac{p_{zg}}{n_z}, \quad \forall c \in \mathcal{C}, g \in \mathcal{G}, \tag{1}$$

where p_{zg} is the probability of fault zone z being activated and causing a PGA of g. However, any city c will also be contingent on other cities geographically, which means that the hazard of an earthquake in any city s will also add to the total hazard of city c by a factor relative to the distance between them. We define the contingency between any two cities c and s in terms of their proximity and using an arbitrary function of the Euclidean distance d_{cs} as follows:

$$Co_{cs} = \frac{1}{2^{d_{cs}}}, \quad \forall c \in \mathcal{C}, s \in \mathcal{S}. \tag{2}$$

Note that the choice of Co_{cs} is not our primary concern and the framework can accommodate any reasonable function. Further discussion on the relation between PGA and distance can be found in [32] and the references therein. To illustrate; if the distance between two (not necessarily adjacent cities) is 200 miles, then an earthquake of demand parameter g in city s is assumed to be felt as an earthquake of size $0.25g$ in city c. In other words, the hazard of city s being epicenter to an earthquake of size g will contribute to the total hazard in city c for an earthquake of the same size by 25%. The hazard in city c for being affected from an earthquake of size g in city s can then be written as

$$H_{csg} = Co_{cs}EP_{sg}, \quad \forall c \in \mathcal{C}, s \in \mathcal{S}, g \in \mathcal{G}. \tag{3}$$

Note that (3) boils down to EP_{cg} for any city that hosts the eartquake. Integrating over all scenarios, we can find the cumulative hazard in city c as

$$H_{cg} = \sum_{s} H_{csg} = \sum_{s} Co_{cs}EP_{sg} = EP_{cg} + \sum_{s \neq c} Co_{cs}EP_{sg}, \quad \forall c \in \mathcal{C}, s \in \mathcal{S}, g \in \mathcal{G}. \tag{4}$$

Therefore, the cumulative hazard of city c is the probability that city c will be the epicenter of the next devastating earthquake, plus the sum of the same probabilities for other cities in $\mathcal{C}$ adjusted by a factor of geographical contingency.

As stated previously, the level of damage from an earthquake is determined collectively by its hazard together with the vulnerability of infrastructure as well as exposure of property stock. Given an earthquake of parameter g occurs in city c, the probabilistic vulnerability (i.e., conditional probability that the building stock in city c will exceed the *complete damage* or *collapse* threshold d_0) is determined by a fragility curve [33] and can be stated as

$$VP_{cg} = P_c(D > d_0 | G = g), \quad \forall c \in \mathcal{C}, g \in \mathcal{G}. \tag{5}$$

Therefore, given the building stock in city c is S_c, the expected number of buildings in city c reaching the complete damage state (i.e., collapse) given a devastating earthquake occurs can be computed as

$$V_{cg} = VP_{cg}S_c, \quad \forall c \in \mathcal{C}, g \in \mathcal{G}, \tag{6}$$

where, again, the conditional probability of collapse given the earthquake demand parameter g, V_{cg}, is recovered from the vulnerability curve that is specific to city c. Figure 3 illustrates sample curves which are constructed from log-normal CDFs with arbitrary μ values ranging from 0 to 1, and $\sigma = 0.5$. A discussion of the calibration of these curves to real earthquake data is beyond the scope of our work and can be found in [33] or [34]. Note that the fragility curves depicted here reflect varying vulnerability levels only for a single damage state, i.e., complete damage, which will be our focus in this study.[2]

Therefore, the risk of city c from a disaster due to an earthquake of size g in city s, that is, the expected number of buildings in city c reaching the total damage state, can be expressed as

$$R_{csg} = H_{csg}V_{cg}, \quad \forall c \in \mathcal{C}, s \in \mathcal{S}, g \in \mathcal{G}. \tag{7}$$

Summing over all possible size-location scenarios, we state the overall risk from an earthquake

2 In general, fragility curves are used to depict the conditional probability of exceeding certain damage levels for a given vulnerability level.

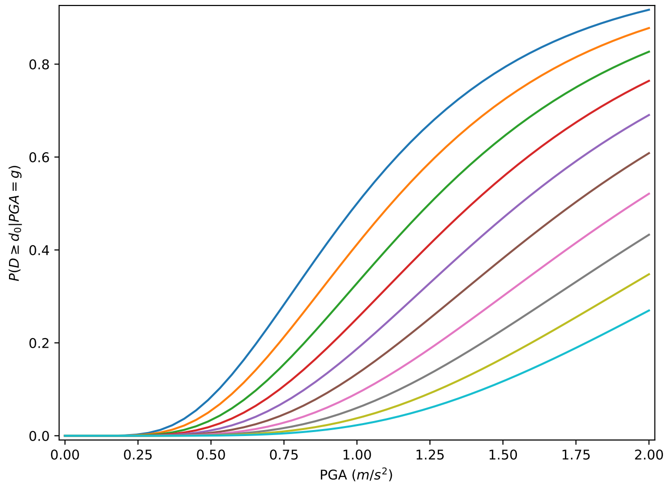

Figure 3. Probabilistic vulnerability curves (only the total damage state)

disaster in city c as

$$R_c = \sum_{s,g} R_{csg}, \quad \forall c \in \mathcal{C}. \tag{8}$$

Note that the risk values already incorporate the contingencies through the hazard values H. Given the seismic risk framework above, the expected demand of city c for SAR unit type k can be determined by the equation

$$\mathbb{E}\left[DM_{ck}\right] = \alpha_k R_c, \quad \forall c \in \mathcal{C}, k \in \mathcal{K}. \tag{9}$$

Since devastating earthquakes are considered as low-probability events (although with extreme conditional damage), one challenging task for the policymakers and relevant authorities is to determine the appropriate number of SAR units to keep ready because it is not rational for governments to ensure the availability of SAR units in an anticipation of the worst-case scenario (*vulnerability-based approach*) by setting

$$Av_k = \max_{s,g} \left\{ \alpha_k \sum_c \left(\frac{H_{csg}}{EP_{sg}} \right) V_{cg} \right\} = \max_{s,g} \left\{ \alpha_k \sum_c Co_{sc} V_{cg} \right\}, \quad \forall k \in \mathcal{K}. \tag{10}$$

On the contrary, taking a solely *risk-based approach* such that

$$Av_k = \alpha_k \sum_c R_c = \sum_c \mathbb{E}\left[DM_{ck}\right] = \mathbb{E}\left[DM_k\right], \quad \forall k \in \mathcal{K}, \tag{11}$$

would again be unrealistic as it will overlook the devastating conditional impact of severe earthquakes. In this paper, acknowledging the fact that predicting the size and/or location of an earthquake is much more difficult than predicting whether or not an earthquake will occur, we suggest that countries with high risks of earthquake can take a *conditional-risk-based approach* by assuming that there will be definitely an earthquake and basing their provision policies on the conditional risk of an earthquake (i.e., given one of the cities becomes an epicenter with certainty):

$$\begin{aligned} Av_k = \mathbb{E}\left[DM_k|EP\right] &= \alpha_k \frac{\sum_c R_c}{\sum_{s,g} EP_{sg}} \\ &= \alpha_k \frac{\sum_{c,s,g} Co_{cs} EP_{sg} V_{cg}}{\sum_{s,g} EP_{sg}} = \alpha_k \sum_{c,s,g} Co_{cs} V_{cg} EP_{sg|EP}, \quad \forall k \in \mathcal{K}, \end{aligned}$$

where we introduced the conditional probability of city s being an epicenter to an earthquake of size g (given there is an earthquake) as

$$EP_{sg|EP} := \frac{EP_{sg}}{EP}, \quad \forall s \in \mathcal{S}, g \in \mathcal{G}, \tag{12}$$

with $EP = \sum_{s,g} EP_{sg}$. To summarize the three approaches,

i. *Vulnerability-based approach:* the worst-case scenario will happen with probability one.
ii. *Risk-based approach:* whether, where and at which size an earthquake will occur should be handled as an expected value.
iii. *Conditional-risk-based approach:* an earthquake will definitely happen, but we don't know where it will happen and at which size.

Vulnerability-adjusted fastest routes via RL: a DP approach

As an input to the mathematical optimization model to be discussed in Section 3, we also recover the fastest route between any two cities on the grid that takes into account accessibility during an earthquake using a DP approach. The explicit enumeration approach offers a relatively poor runtime performance on larger grids (e.g., it can take long hours to enumerate all paths on a 5x5 grid).

Given an earthquake of size g occurs in city s, the vulnerability-adjusted travel time of SAR unit type k between two adjacent cities c and c' is introduced as

$$\tilde{T}_{cc'ksg} = \frac{d_{cc'}}{v_k\left(1 - \frac{H_{csg} VP_{cg} + H_{c'sg} VP_{c'g}}{2}\right)} = \frac{d_{cc'}}{\tilde{v}_{cc'ksg}}, \quad \forall c, c' \in \mathcal{C}, k \in \mathcal{K}, s \in \mathcal{S}, g \in \mathcal{G}, \tag{13}$$

where $\tilde{v}_{cc'ksg}$ can be considered as the vulnerability-adjusted speed of unit type k between cities c and c' should there be an earthquake of size g in city s. It is obvious from Eq. (13) that if the probabilistic vulnerabilities of any pairs of cities (c, c') get closer to 1, then $\tilde{v}_{cc'ksg}$ will get close to 0, meaning that the route will be unusable.

We formulate the fastest route problem using the DP approach [35]. A policy π is the probabilities assigned to a certain set of actions $a \in \mathcal{A}$ (moves on the grid map in our case) for each state $c \in \mathcal{C}$. In particular, $\pi_{sg}(a|c)$ is the probability that the SAR entity will choose to make one of the eight possible moves ($\uparrow \nearrow \rightarrow \searrow \downarrow \swarrow \leftarrow \nwarrow$) given it is currently in city c. The value of an action a in city c under policy π (or the city-action value), denoted by $v^\pi(a|c)$, is determined by the sum of the immediate reward from transitioning to city c', denoted by $r(c'|c)$, and the continuation value $v^\pi(c')$

$$v^\pi_{sg}(c, a) = \sum_{c'} p(c'|c, a)\left(r_{sg}(c'|c) + v^\pi_{sg}(c')\right), \quad \forall s \in \mathcal{S}, g \in \mathcal{G}, \tag{14}$$

where $p(c'|c,a)$ is the probability of ending up in city c' by taking move a in city c (which is obviously 1 for the city in the direction of the move and 0 for others in our case). We set $r_{sg}(c'|c) = -\tilde{T}_{cc'ksg}$ depending on the equipment type k. Integrating (14) over all possible actions (each with appropriate probabilities $\pi(a|c)$ yields the city value function

$$v_{sg}^{\pi}(c) = \sum_{c'} p(c'|c)\left(r_{sg}(c'|c) + v_{sg}^{\pi}(c')\right), \quad \forall s \in \mathcal{S}, g \in \mathcal{G}, \tag{15}$$

where $p(c'|c) = \sum_{a \in \mathcal{A}} p(c'|c,a)\pi_{sg}(a|c)$. The optimal policy is then the one that maximizes the value of being in each city:

$$\pi_{sg}^{*} = \arg\max_{\pi} v_{sg}^{\pi}(c), \quad \forall c \in \mathcal{C}, s \in \mathcal{S}, g \in \mathcal{G}. \tag{16}$$

The search for π_{sg}^{*} involves two steps, namely, policy evaluation and policy iteration (improvement). Evaluation of an arbitrary policy is a recursive operation that runs until the value of $v_{\pi}(c)$ stabilizes across all cities. At each step, the value of $v^{\pi}(c)^{sg}$ is calculated by evaluating all possible actions for all cities through $v_{sg}^{\pi}(c,a)$. At policy iteration step, the policy is updated based on the re-calculated values of $v_{sg}^{\pi}(c)$ and $v_{sg}^{\pi}(c,a)$, $\forall c \in \mathcal{C}, a \in \mathcal{A}$.

As an example, the calculated values of the city value function as well as the corresponding optimal routes and travel times on a 4x4 grid for various endpoints, SAR unit types, scenarios and earthquake sizes are shown in Figure 4.

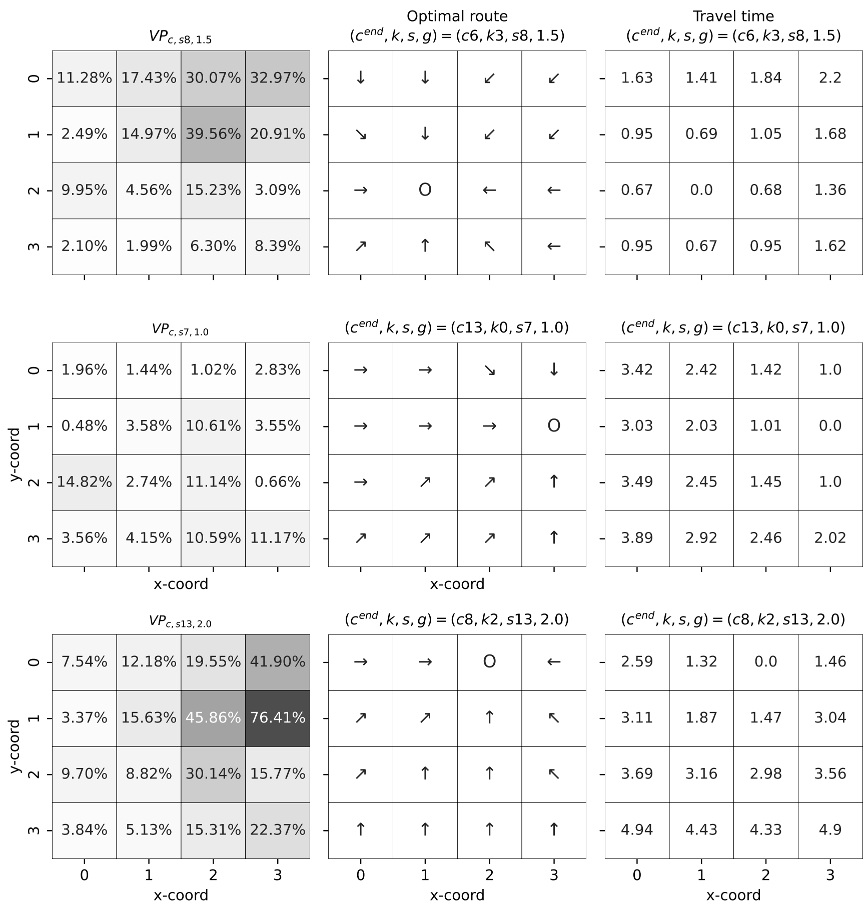

Figure 4. Percentage vulnerabilities (left), optimal routes (middle) and shortest travel times (right) on a 4x4 grid for different end-points and values of k, s, g

MINLP model variables, objectives and constraints

Decision and non-decision variables of the MINLP model and their explanations are provided in Table 5-Table 6.

Table 5. Decision variables defined in the MINLP model

$Z_{fk} \in \{0,1\}$	whether a facility f for SAR unit type k is established or not
$X_{fk} \in \mathbb{Z}^+$	amount of SAR unit type k to be allocated to facility f
$Y_{fcksg} \in \mathbb{Z}^+$	amount of SAR unit type k to be dispatched from facility f to city c in an earthquake of size g in city s

Table 6. Non-decision variables defined in the MINLP model

T_{ksg}	average dispatch time of SAR unit type k in an earthquake of size g in city s
T_{sg}^{max}	maximum average dispatch time across SAR unit types in an earthquake of size g in city s
T^{max}	Expected maximum average dispatch time
$Fulfill_{cksg} \in [0,1]$	proportion of demand by city c for SAR unit type k fulfilled given an earthquake of size g occurs in city s
$Fulfill_{ck} \in [0,1]$	expected proportion of demand by city c for SAR unit type k fulfilled
$Fulfill_{ksg} \in [0,1]$	proportion of demand for SAR unit type k fulfilled given an earthquake of size g occurs in city s
$Fulfill_k \in [0,1]$	expected proportion of demand for SAR unit type k fulfilled

Our two main objectives in this model is to minimize (i) the expected upper bound for the average dispatch time of SAR units taking into account all size-location scenarios, and (ii) the expected mean absolute deviation across fulfillment rates of cities. This will also help us minimize preventable humanitarian losses, as the survival rate is generally considered to be a decreasing function of time. To this end, we define the average time it takes to dispatch SAR unit type k under any scenario as the vulnerability-adjusted dispatch times between all facility-city pairs, $\tilde{T}_{fcksg}$, weighted by the percentage of flow:

$$T_{ksg} = \sum_{f,c} \tilde{T}_{fcksg} \frac{Y_{fcksg}}{\sum_{f,c} Y_{fcksg}}, \quad \forall k \in \mathcal{K}, s \in \mathcal{S}, g \in \mathcal{G}. \tag{17}$$

So, on average, all demand for SAR unit type k will have arrived at earthquake sites in T_{ksg} hours, should there be any earthquake of size g in city s. Since we assume that SAR units are interdependent (e.g., rescue teams on excavators, excavators on ambulances, ambulances on rescue teams), our aim is the minimize, in each scenario, the maximum of the average times across all cities for equipment type k, which is defined as

$$T_{sg}^{max} = \max \left\{ T_{ksg} : k \in \mathcal{K} \right\}, \quad \forall s \in \mathcal{S}, g \in \mathcal{G}. \tag{18}$$

Expected maximum dispatch time is then the average of the maximum dispatch times T_{sg}^{max} weighted by the possibility of a given scenario:

$$T^{max} = \sum_{s,g} T_{sg}^{max} EP_{sg|EP}. \tag{19}$$

Accordingly, we can state our first objective as

$$\min \quad \theta_1 = T^{max}. \tag{20}$$

Our second objective will ensure the fair distribution of SAR assets by minimizing the mean absolute deviation of fulfillment rate for each city from the average fulfillment rate under each size-location scenario. The rate of fulfillment of demand from each city for SAR unit type k under scenario (s, g) is given by

$$Fulfill_{cksg} = \frac{\sum_f Y_{fcksg}}{DM_{cksg}}, \quad \forall c \in \mathcal{C}, k \in \mathcal{K}, s \in \mathcal{S}, g \in \mathcal{G}, \tag{21}$$

fulfillment of demand from each city for SAR unit type k is then the average of $Fulfill_{cksg}$ values weighted by the conditional probability of each scenario:

$$Fulfill_{ck} = \sum_{s,g} Fulfill_{cksg} EP_{sg|EP}, \quad \forall c \in \mathcal{C}, \forall k \in \mathcal{K}. \tag{22}$$

Similary, fulfillment of demand for SAR unit type k, both under each scenario and on average, can be expressed as

$$Fulfill_{ksg} = \frac{\sum_{f,c} Y_{fcksg}}{\sum_c DM_{cksg}}, \quad \forall k \in \mathcal{K}, s \in \mathcal{S}, g \in \mathcal{G}, \tag{23}$$

$$Fulfill_k = \sum_{s,g} Fulfill_{ksg} EP_{sg|EP}, \quad \forall k \in \mathcal{K}. \tag{24}$$

We then state mean absolute deviation for each size-location scenario and expected mean absolute deviation as

$$Fulfill^{\text{dev}}_{ksg} = \frac{\sum_c \left| Fulfill_{cksg} - Fulfill_{ksg} \right|}{|\mathcal{C}|)}, \quad \forall k \in \mathcal{K}, s \in \mathcal{S}, g \in \mathcal{G}, \tag{25}$$

and

$$Fulfill^{\text{dev}}_k = \sum_{s,g} Fulfill^{\text{dev}}_{ksg} EP_{sg|EP}, \quad \forall k \in \mathcal{K}, \tag{26}$$

respectively. Our second objective is therefore

$$\min \quad \theta_2 = Fulfill^{\text{dev}}_{k_0 sg}. \tag{27}$$

In Eq. (27), we were able to change k to k_0 (i.e., SAR unit type 0) because availability of SAR units, and deployment to cities under each scenario, namely, Av_k and Y_{fcksg}, are proportional among SAR unit types (recall the *interdependence* argument).

On the other hand, we deal with the bi-objectiveness of the MINLP model by applying the weighted sum over the deviations of objectives given in Eq. (20) and Eq. (27) from their respective best possible values, scaled by the difference between their respective best and worst values $\underline{\theta}$ and $\overline{\theta}$:

$$\min \quad \theta = w\left(\frac{\theta_1 - \underline{\theta}_1}{\overline{\theta}_1 - \underline{\theta}_1}\right) + (1-w)\left(\frac{\theta_2 - \underline{\theta}_2}{\overline{\theta}_2 - \underline{\theta}_2}\right). \tag{28}$$

Before implementing the objective (28), the model is first solved as single-objective for (20) to obtain best and worst values for θ_1 and θ_2, respectively, and then for (27) to obtain the best and worst values for θ_2 and θ_1, again, respectively.

Having defined the decision variables and objective functions, we can now express the constraints of the model to be satisfied while achieving the objective (28). First, we require all $\bar{T}_{ksg}$ values to be less than or equal to their supremum T_{sg}^{max}:

$$T_{ksg} \leq T_{sg}^{max}, \quad \forall k \in \mathcal{K}, s \in \mathcal{S}, g \in \mathcal{G}. \tag{29}$$

The total number of facilities for each SAR unit type should not exceed the allowed quantity:

$$\sum_f Z_{fk} \leq n_F^k, \quad \forall k \in \mathcal{K}. \tag{30}$$

Furthermore, decision-makers need to make sure that all available equipment is allocated to the facilities and, if allocated, that the facility is established:

$$\sum_f X_{fk} = Av_k, \quad \forall k \in \mathcal{K}, \tag{31}$$

$$X_{fk} \leq MZ_{fk}, \quad \forall f \in \mathcal{F}, k \in \mathcal{K}, \tag{32}$$

where M is a sufficiently large number. Amount of dispatch from facilities to earthquake sites should not exceed the respective capacities of those facilities:

$$\sum_c Y_{fcksg} \leq Z_{fk} X_{fk}, \quad \forall f \in \mathcal{F}, k \in \mathcal{K}, s \in \mathcal{S}, g \in \mathcal{G}. \tag{33}$$

If the sum of equipment k allocated to facilities is less than or equal to the total demand under any scenario, then the total amount of dispatch to earthquake sites should be equal to the amount available (otherwise, it should be equal to the demand), namely,

$$\sum_f X_{fk} \geq \sum_c DM_{cksg} \Longrightarrow \sum_{f,c} Y_{fcksg} = \sum_c DM_{cksg}, \quad \forall k \in \mathcal{K}, s \in \mathcal{S}, g \in \mathcal{G},$$

and

$$\sum_{f \in \mathcal{F}} X_{fk} < \sum_{c \in \mathcal{C}} DM_{cksg} \Longrightarrow \sum_{f,c} Y_{fcksg} = \sum_f X_{fk}, \quad \forall k \in \mathcal{K}, s \in \mathcal{S}, g \in \mathcal{G}.$$

In other words, amount of total deployment of SAR unit type k under each scenario should be the minimum among the available and demanded amount of SAR units of type k:

$$\sum_{f,c} Y_{fcksg} = \min \left\{ \sum_{f} X_{fk}, \sum_{c} DM_{cksg} \right\}, \quad \forall k \in \mathcal{K}, s \in \mathcal{S}, g \in \mathcal{G}. \tag{34}$$

We linearize Eq. (34) to improve runtime.[3]
Amount of SAR units dispatched to any city should not exceed its demand under any scenario:

$$\sum_{f} Y_{fcksg} \leq DM_{cksg}, \quad \forall c \in \mathcal{C}, k \in \mathcal{K}, s \in \mathcal{S}, g \in \mathcal{G}. \tag{35}$$

Finally, the deployment of SAR units should preserve proportionality since they are interdependent:

$$\sum_{f} Y_{fcksg} = \alpha_k \sum_{f} Y_{fck_0sg}, \quad \forall c \in \mathcal{C}, k \in \{\mathcal{K} \setminus k_0\}, s \in \mathcal{S}, g \in \mathcal{G}. \tag{36}$$

The allocation-dispatchment model described through Eqs. (28)-(36) is obviously non-linear, with the non-linearity arising from the two objectives, namely, due to the maximum function in Eq. (18) and ratio of decision variables in Eq. (27). The non-linearity in Eq. (18) is eliminated through constraint (29). Handling Eq. (27) requires transformation of model variables, which is not straightforward. A further non-linearity is imposed by Eq. (34), which is also substituted with linear constraints. The remaining non-linearity, coupled with large number of constraints and arbitrarily generated initial problem settings, manifests itself high computation times (see Section 5). The comprehensive model presented throughout this section will be applied to a hypothetical example in Section 4 where we will also present some analysis of results and policy insights.

4 A numerical example

The numerical example presented in this section aims to illustrate the seismic-risk-based resource allocation and dispatch framework through a minimal example but is flexible enough to extend to cover higher-dimensional scenarios. Figure 5 (panels *i*-*vi*) displays the main components of the

3 This is done by representing Eq. (34) by the following constraints and restrictions:

$$\begin{aligned}
\sum_{f} X_{fk} &\geq \sum_{c} DM_{cksg} + M(u_{ksg} - 1), && \forall k \in \mathcal{K}, s \in \mathcal{S}, g \in \mathcal{G}, \\
\sum_{c} DM_{cksg} + M(u_{ksg} - 1) \leq \sum_{f,c} Y_{fcksg} &\leq \sum_{c} DM_{cksg} + M(1 - u_{ksg}), && \forall k \in \mathcal{K}, s \in \mathcal{S}, g \in \mathcal{G}, \\
\sum_{f} X_{fk} + \epsilon &\leq \sum_{c} DM_{cksg} + M(1 - u'_{ksg}), && \forall k \in \mathcal{K}, s \in \mathcal{S}, g \in \mathcal{G}, \\
\sum_{f} X_{fk} + M(u'_{ksg} - 1) \leq \sum_{f,c} Y_{fcksg} &\leq \sum_{f} X_{fk} + M(1 - u'_{ksg}), && \forall k \in \mathcal{K}, s \in \mathcal{S}, g \in \mathcal{G}, \\
u_{ksg} + u'_{ksg} &= 1, && \forall k \in \mathcal{K}, s \in \mathcal{S}, g \in \mathcal{G}, \\
u_{ksg}, u'_{ksg} &\in \{0, 1\}, && \forall k \in \mathcal{K}, s \in \mathcal{S}, g \in \mathcal{G}.
\end{aligned}$$

seismic hazard framework based on expectations.[4] There are 4 fault zones in the map (*i-ii*) and these zones can trigger earthquakes with assigned probabilities (*iii*). Together with contingencies, these probabilities constitute the overall hazard of earthquake (*iv*). Combined with percentage vulnerabilities for different demand parameters derived from fragility curves given in Figure 3, the level of exposure determines the risk of a disaster (*vi*).

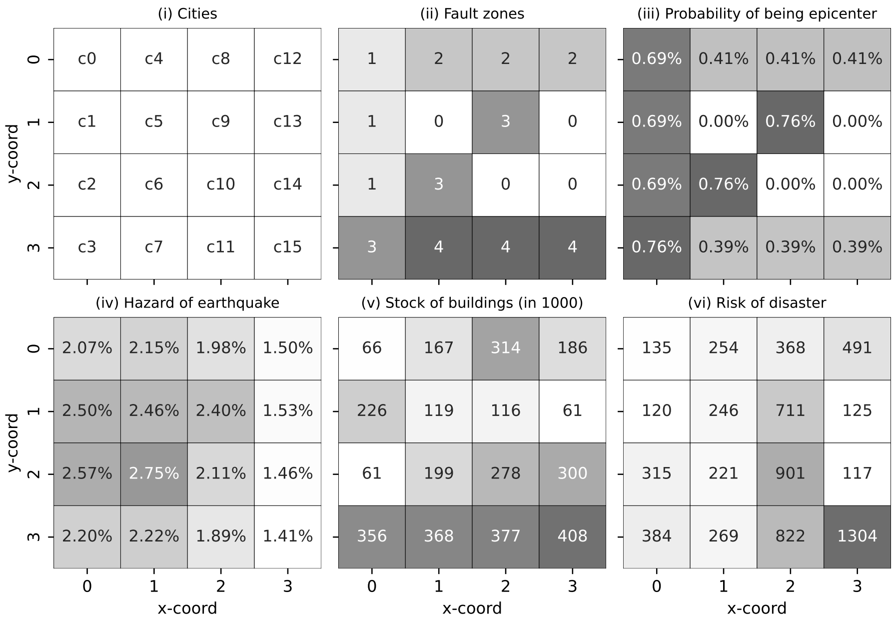

Figure 5. Main components of the seismic hazard framework

Figure 6, on the other hand, demonstrates a realized scenario, namely, $s = s_2$ and $g = 2.0$ (that is, an earthquake of size 2.0 occurs in city 2). Now, since the hazard is realized, the hazard map turns into a realized hazard map where the impact propagates based on distances. From the realized risk map (*iv*), we can see how many collapses this scenario can cause in different cities based on their vulnerabilities (*ii*) and building stocks (*iii*).

The optimization model presented in Section 3 is implemented using Gurobi solver on a workstation with an Intel(R) Xeon(R) W-2245 CPU @ 3.90GHz processor with a 64.0GB installed RAM. Figure 7 displays the optimal allocation of equipment type k_0 for $n_F = 7$ (top left), as well as conditional risk levels (top right), average dispatch times (bottom left) and fulfillment rates (bottom right) for a single scenario (i.e., $s = s_6$, $g = 1.0$) where we also arbitrarily set $w = 0.5$. Figure 8 illustrates the deployment plan for the sample scenario. The overall fulfillment rate for k_0 under this allocation plan is calculated as 83.4%. Expected fulfillment rates across cities for $n_F^k = 7\ \forall k$ are depicted in Figure 9 where we observe a small variation (thanks to our second objective function θ_2). For $w = 0.5$ and $n_F^k = 7\ \forall k$, the optimal values of θ_1 and θ_2 are calculated as 0.8281 hours and 0.025%. We present results for some more scenarios in Table 7.

We extend these results through a number sensitivity analyses based on two key model parameters, namely, the maximum number of facilities for SAR unit type k, n_F^k, and the objective weight factor, w. Figure 10 displays the sensitivity of each objective function value with respect to these two parameters whereas Table 7 presents these results in numerical format. As expected, optimal value

4 For reproducibility, we use seed 51 in Python's NumPy library, which is chosen as it yielded a lower computation time.

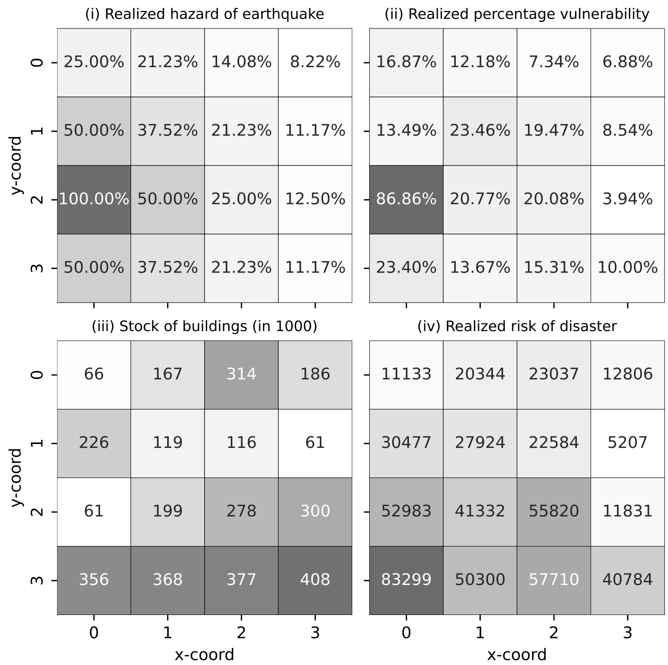

Figure 6. Main components of the seismic hazard framework (a realized scenario with $s = s_2$ and $g = 2.0$)

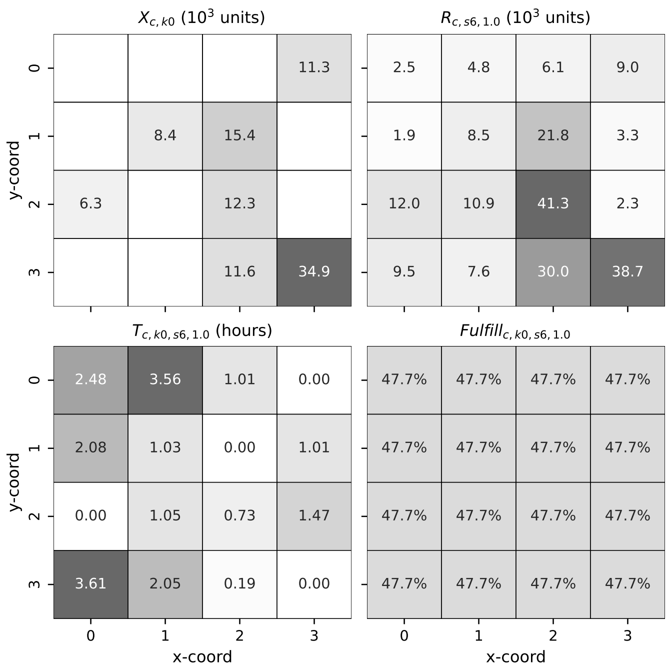

Figure 7. Optimal allocation of SAR unit type k_0 for $n_F = 7$ (top left), as well as realized risk (top right), average dispatch times (bottom left) and fulfillment rates (bottom right) for $s = s_6, g = 1.0$

of the expected maximum deployment time decreases with the number of allowed facilities (left). The impact of the latter on mean absolute deviation of fulfillment rates is somewhat reverse (mid). Increasing the number of facilities somehow worsens the optimal value of θ_2, leading to a higher deviation across fulfillment rates. As far as the main objective function θ is concerned (right), we can observe that the total percentage deviation from the two goals peaks at $(w, n_F) = (0.75, 6)$ with 6.98%. The sensitivity analyses can assist decision-makers in choosing the optimal number of facilities and devising an allocation-dispatchment plan. For example, if the primary focus is

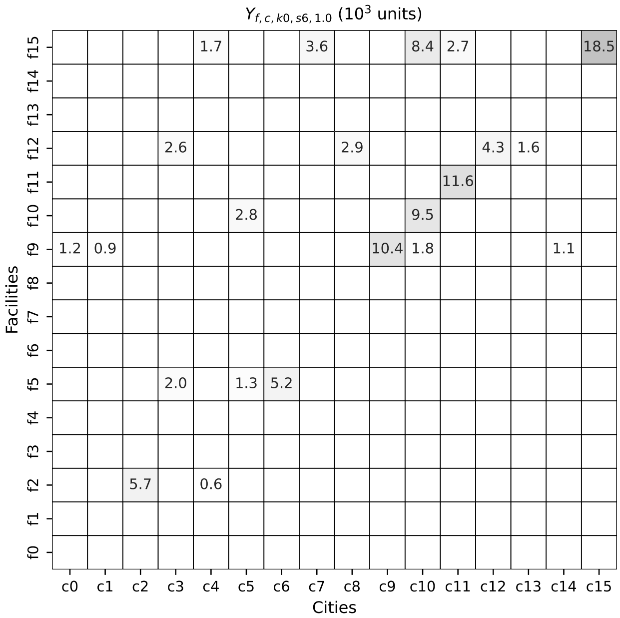

Figure 8. Optimal dispatching of SAR unit type k_0 for $n_F = 7$ and a single scenario ($s = s_6, g = 1.0$)

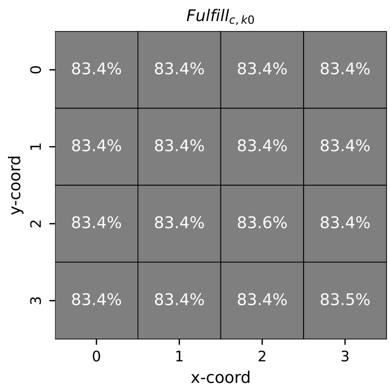

Figure 9. Expected fulfillment rate for SAR unit type k_0 and $n_F = 7$

on the speed of dispatchment, then the choice of $(w, n_F) = (1, 7)$ yields an expected maximum deployment time of as low as 0.3514 hours, although with an expected mean deviation of 10.94%. Or, if the policymakers are of the view that the deployment speed is three times as important as having an equitable deployment, namely, $(w, n_F) = (0.75, 7)$, then a 0.67% expected deviation can be achieved with an increase in expected maximum dispatch time to 0.6859 hours (again, Table 7).

5 Results and discussion

In real earthquake situations, survival rate is largely determined by the speed of intervention, whereas poor planning can result in the clustering of available resources in a subset of affected locations, resulting in an inequitable situation for victims. Recent big earthquakes, such as the two that struck 11 cities in southern Turkey in 2023, has shown that it is not the abundance of resources that matters for the well-functioning of disaster response but how these resources are pre-positioned and deployed.

Results from hypothetical examples (including the one presented in Section 4) indicate that the seismic-risk-based bi-objective MINLP model is feasible under various risk scenarios and can be

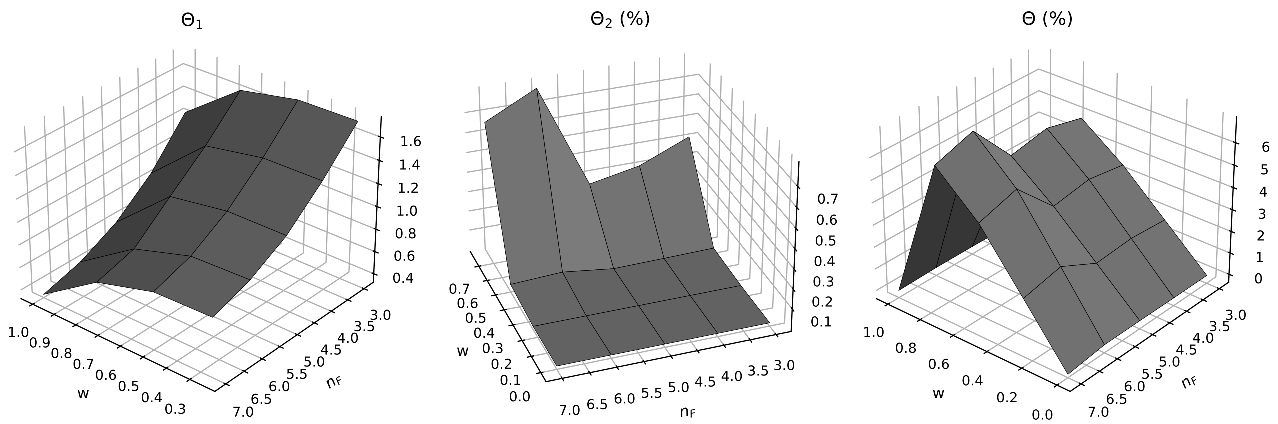

Figure 10. Sensitivity of objective values $\theta, \theta_1, \theta_2$ with respect to n_F and w

Table 7. Optimal values for various w and n_F

		n_F				
w		3	4	5	6	7
0	θ_1	8,0135	6,7374	7,5972	7,0617	8,0135
	θ_2	0,00%	0,00%	0,00%	0,00%	0,00%
	θ	-0,01%	-0,01%	0,00%	-0,01%	-0,23%
0.25	θ_1	1,7402	1,4128	1,1352	0,9547	0,8411
	θ_2	0,00%	0,00%	0,00%	0,00%	0,00%
	θ	1,75%	1,88%	1,75%	2,63%	2,25%
0.5	θ_1	1,7333	1,4084	1,1327	0,9363	0,8281
	θ_2	0,01%	0,01%	0,01%	0,04%	0,03%
	θ	3,51%	3,78%	3,50%	5,23%	4,70%
0.75	θ_1	1,6320	1,3171	1,0527	0,7811	0,6859
	θ_2	0,43%	0,32%	0,27%	0,80%	0,67%
	θ	4,91%	5,33%	5,00%	6,98%	6,40%
1	θ_1	1,2527	0,8765	0,6148	0,4470	0,3514
	θ_2	12,79%	12,24%	11,80%	11,30%	10,94%
	θ	-0,19%	-0,05%	-0,02%	-0,01%	-0,04%

applied to make allocation-deployment decisions when the size and location of earthquakes are uncertain. With equal weights for two objectives, the model achieves a total of 3.5% deviation from single-objective solutions (more precisely, the difference between negative and positive ideal solutions) with an expected maximum dispatch time of 1.1327 hours and expected mean absolute deviation of 0.01%. Sensitivity analysis results, on the other hand, verify that the model behaves in accordance with our expectations as far as the changes in the number of allowed facilities and weights of individual objectives are concerned.

Yet, the ability of the model to adapt to different problem sizes is hindered by rapidly growing computational complexity and runtimes, which is illustrated in Table 8.

Table 8. DP and MINLP model runtimes for different problem sizes (random seed: 51)

Grid size	DP runtime (sec, per scenario)	DP runtime (sec, total)	Number of constraints	MINLP model runtime (sec)
3x3	0.13	4.7	9,417	6.4
4x4	0.90	57.6	27,029	350
5x5	4.09	409	62,921	5,469

6 Conclusion

This paper sought to develop an integrated and versatile framework for SAR unit pre-allocation and deployment, incorporating a seismic risk component similar to the one discussed in [10] into a MINLP model to minimize the dispatch time of SAR units and deviation between response rates. The features of the model introduced in this paper are by no means exhaustive. In particular, the seismic risk framework presented here offers a simple yet flexible approach that can be adapted to various problem sizes and hazard maps, as well as vulnerability and exposure profiles. The bi-objective MINLP model then linked the seismic hazard framework with the resource allocation and dispatchment problem where the vulnerability-(or conditional-risk-)adjusted shortest routes were recovered from the computationally efficient DP algorithm. The bi-objectiveness of the problem under study is handled through derivation of a pareto optimality surface for the weighted sum of percentage deviations from the individual objectives.
The model's efficiency, however, is mainly limited by the runtime that is exponentially increasing with the problem size. Moreover, lack of a real case study might be concealing the potential hassles in representing real maps as simple grids (e.g., a single node might include multiple cities or vice versa). Besides, various assumptions made in the study (e.g., contingency structure assumed in Eq. (2), uniform distribution of property stock, even probability for any part of a fault line being activated, etc.) might render the model difficult to apply in real life. Thus, as an outlook, acquiring real seismic hazard and exposure data for model validation purposes, working with fragility curves calibrated to observed vulnerabilities, a critical review of the assumptions made through expert solicitations, integrating meta-heuristics for improving computational efficiency for larger problem sizes can further enhance the applicability of the model to real-life situations.

Declarations

Use of AI tools

The author declares that he has not used Artificial Intelligence (AI) tools in the creation of this article.

Data availability statement

There are no external data associated with the manuscript.

Ethical approval (optional)

The author states that this research complies with ethical standards. This research does not involve either human participants or animals.

Consent for publication

Not applicable

Conflicts of interest

The author declares that he has no conflict of interest.

Funding

No funding was received for this research.

Author's contributions

The author has written, read and agreed to the published version of the manuscript.

Acknowledgements

Not applicable

References

[1] World Health Organization (WHO), Earthquakes, (2024). https://www.who.int/health-topics/earthquakes#tab=tab_1

[2] Schweier, C. Geometry based estimation of trapped victims after earthquakes. In Proceedings *International Symposium on Strong Vrancea Earthquakes and Risk Mitigation*, pp. 4-6, Bucharest, Romania, (2007, October).

[3] Weber, M. Rural areas may suffer disproportionately in quakes. *Temblor,* (2020). [CrossRef]

[4] Noji, E.K. The public health consequences of disasters. *Prehospital and Disaster Medicine*, 15(4), 21-31, (2000). [CrossRef]

[5] Kunkle, R. Medical care of entrapped patients in confined spaces. In Proceedings, *International Workshop on Earthquake Injury Epidemiology: Implications for Mitigation and Response*, pp. 338-344, Baltimore, Maryland, USA, (1989, July). [CrossRef]

[6] Ahmadi, G., Tavakkoli-Moghaddam, R., Baboli, A. and Najafi, M. A decision support model for robust allocation and routing of search and rescue resources after earthquake: a case study. *Operational Research*, 22, 1039–1081, (2022). [CrossRef]

[7] Klibi, W., Ichoua, S. and Martel, A. Prepositioning emergency supplies to support disaster relief: a case study using stochastic programming. *INFOR: Information Systems and Operational Research*, 56(1), 50-81, (2018). [CrossRef]

[8] Chiu, Y.Y., Omura, H., Chen, H.E. and Chen, S.C. Indicators for post-disaster search and rescue efficiency developed using progressive death tolls. *Sustainability*, 12(19), 8262, (2020). [CrossRef]

[9] Condeixa, L.D., Leiras, A., Oliveira, F. and De Brito Jr, I. Disaster relief supply pre-positioning optimization: A risk analysis via shortage mitigation. *International Journal of Disaster Risk Reduction*, 25, 238-247, (2017). [CrossRef]

[10] Arnette, A.N. and Zobel, C.W. A risk-based approach to improving disaster relief asset pre-positioning. *Production and Operations Management*, 28(2), 457-478, (2019). [CrossRef]

[11] Caunhye, A.M., Nie, X. and Pokharel, S. Optimization models in emergency logistics: A literature review. *Socio-Economic Planning Sciences*, 46(1), 4-13, (2012). [CrossRef]

[12] Kaveh, A., Javadi, S.M. and Moghanni, R.M. Emergency management systems after disastrous earthquakes using optimization methods: A comprehensive review. *Advances in Engineering Software*, 149, 102885, (2020). [CrossRef]

[13] Boonmee, C., Arimura, M. and Asada, T. Facility location optimization model for emergency humanitarian logistics. *International Journal of Disaster Risk Reduction*, 24, 485-498, (2017). [CrossRef]

[14] Chen, L. and Miller-Hooks, E. Optimal team deployment in urban search and rescue. *Transportation Research Part B: Methodological*, 46(8), 984-999, (2012). [CrossRef]

[15] Döyen, A., Aras, N. and Barbarosoğlu, G. A two-echelon stochastic facility location model for humanitarian relief logistics. *Optimization Letters*, 6, 1123-1145, (2012). [CrossRef]

[16] Zhang, L., Liu, T. and Huang, J. Relief equipment layout model for natural disaster with uncertain demands. In Proceedings, *2009 International Conference on Management and Service*

Science, pp. 1-4, Beijing, China, (2009, September). [CrossRef]

[17] Ghasemi, P., Khalili-Damghani, K., Hafezalkotob, A. and Raissi, S. Stochastic optimization model for distribution and evacuation planning (A case study of Tehran earthquake). *Socio-Economic Planning Sciences*, 71, 100745, (2020). [CrossRef]

[18] Mohammadi, R., Ghomi, S.F. and Jolai, F. Prepositioning emergency earthquake response supplies: A new multi-objective particle swarm optimization algorithm. *Applied Mathematical Modelling*, 40(9-10), 5183-5199, (2016). [CrossRef]

[19] Paul, J.A. and MacDonald, L. Location and capacity allocations decisions to mitigate the impacts of unexpected disasters. *European Journal of Operational Research*, 251(1), 252-263, (2016). [CrossRef]

[20] Zhang, S., Guo, H., Zhu, K., Yu, S. and Li, J. Multistage assignment optimization for emergency rescue teams in the disaster chain. *Knowledge-Based Systems*, 137, 123-137, (2017). [CrossRef]

[21] Vahdani, B., Veysmoradi, D., Shekari, N. and Mousavi, S.M. Multi-objective, multi-period location-routing model to distribute relief after earthquake by considering emergency roadway repair. *Neural Computing and Applications*, 30, 835-854, (2018). [CrossRef]

[22] Khayal, D., Pradhananga, R., Pokharel, S. and Mutlu, F. A model for planning locations of temporary distribution facilities for emergency response. *Socio-Economic Planning Sciences*, 52, 22-30, (2015). [CrossRef]

[23] Sebatli, A., Cavdur, F. and Kose-Kucuk, M. Determination of relief supplies demands and allocation of temporary disaster response facilities. *Transportation Research Procedia*, 22, 245-254, (2017). [CrossRef]

[24] Aghaie, S. and Karimi, B. Location-allocation-routing for emergency shelters based on geographical information system (ArcGIS) by NSGA-II (case study: Earthquake occurrence in Tehran (District-1)). *Socio-Economic Planning Sciences*, 84, 101420, (2022). [CrossRef]

[25] Tirkolaee, E.B., Aydın, N.S., Ranjbar-Bourani, M. and Weber, G.W. A robust bi-objective mathematical model for disaster rescue units allocation and scheduling with learning effect. *Computers & Industrial Engineering*, 149, 106790, (2020). [CrossRef]

[26] Wex, F., Schryen, G., Feuerriegel, S. and Neumann, D. Emergency response in natural disaster management: Allocation and scheduling of rescue units. *European Journal of Operational Research*, 235(3), 697-708, (2014). [CrossRef]

[27] Fiedrich, F., Gehbauer, F. and Rickers, U. Optimized resource allocation for emergency response after earthquake disasters. *Safety Science*, 35(1-3), 41-57, (2000). [CrossRef]

[28] Sharif, S.V., Moshfegh, P.H. and Kashani, H. Simulation modeling of operation and coordination of agencies involved in post-disaster response and recovery. *Reliability Engineering & System Safety*, 235, 109219, (2023). [CrossRef]

[29] Chen, W. and Zhang, L. An automated machine learning approach for earthquake casualty rate and economic loss prediction. *Reliability Engineering & System Safety*, 225, 108645, (2022). [CrossRef]

[30] Zhang, L. and Cui, N. Pre-positioning facility location and resource allocation in humanitarian relief operations considering deprivation costs. *Sustainability*, 13(8), 4141, (2021). [CrossRef]

[31] Edrisi, A. and Askari, M. Probabilistic budget allocation for improving efficiency of transportation networks in pre-and post-disaster phases. *International Journal of Disaster Risk Reduction*, 39, 101113, (2019). [CrossRef]

[32] Bommer, J.J., Stafford, P.J., Alarcón, J.E. and Akkar, S. The influence of magnitude range on empirical ground-motion prediction. *Bulletin of the Seismological Society of America*, 97(6), 2152-2170, (2007). [CrossRef]

[33] Menichini, G., Nistri, V., Boschi, S., Del Monte, E., Orlando, M. and Vignoli, A. Calibration of vulnerability and fragility curves from moderate intensity Italian earthquake damage data. *International Journal of Disaster Risk Reduction*, 67, 102676, (2022). [CrossRef]

[34] Lallemant, D., Kiremidjian, A. and Burton, H. Statistical procedures for developing earthquake damage fragility curves. *Earthquake Engineering & Structural Dynamics*, 44(9), 1373-1389, (2015). [CrossRef]

[35] Sutton, R.S. and Barto, A.G. *Reinforcement Learning: An Introduction*. MIT Press: USA, (2018).

Mathematical Modelling and Numerical Simulation with Applications (MMNSA)
(https://dergipark.org.tr/en/pub/mmnsa)

How to cite this article: Aydın, N.S. (2024). A seismic-risk-based bi-objective stochastic optimization framework for the pre-disaster allocation of earthquake search and rescue units. *Mathematical Modelling and Numerical Simulation with Applications*, 4(3), 370-394. https://doi.org/10.53391/mmnsa.1517843